

Supplementary Materials

for

Investigation and Bioorthogonal anticancer activity Enhancement of triphenylphosphine-labile prodrugs of Seleno-Combretastin-4

Authors: Liyuan Hou¹, Wei Huang¹, Jiaqi Cheng, Xuanru Deng, Haoqiang Lai, Zhen Chen, Zepang zhan, Pengju Feng*, Yiqun Li*, Yang Fang*, Tianfeng Chen

Biological experimental section

Cell culture

Human cervical cancer cell lines including Caski, HeLa and Siha, human breast cancer cell lines containing MCF-7 and M231 cells, human vascular endothelial cells HUVEC and normal cell lines including cervical cell (E6/E7) and embryonic lung cells (Wi38) were purchased from American Type Culture Collection (ATCC, Manassas, VA, USA) and incubated in Dulbecco's Modified Eagle's Medium (DMEM)/1640 medium supplemented with 10% fetal bovine serum (FBS) and 1% penicillin-streptomycin in an incubator (5% CO₂) at 37 °C.

Intracellular uptake of TPP in Caski and HUVEC cells

Lipophilic TPP could be easily absorbed in the tumor cells due to its high lipophilicity. Caski and HUVEC cells incubated in 6-cm dish at a density of 1×10^5 cells per well for 24 h, respectively, were treated with triphenylphosphonium (TPP) at a concentration of 5 μ M for different periods. Then, the cells were washed by PBS, digested by pancreatin, centrifuged (1600 rpm, 5 min) and collected. These acquired cells were re-dispersed in PBS, counted the cell density and digested by mixed acid (nitric acid : perchloric acid = 3:1). Finally, the concentration of phosphorus in the cells was measured by using inductively coupled plasma-mass spectrometry (ICP-MS) and then determined intracellular uptake efficacy.

MTT assays for detecting cytotoxicity

Relative viabilities of cancer and normal cells induced by different concentrations of compounds were detected by MTT assay as previously described. Meanwhile, half inhibition concentration (IC_{50}) values of the cells treated for different compounds for 72 h were analyzed by SPSS software.

Moreover, the combined effects of TPP and seleno compounds on the inhibition of cell proliferation were measured. Briefly, cells pre-incubated with TPP for 4 h according to the above results of cellular uptake of TPP, then cultured in DMEM containing different concentrations of SeD and CSeD compounds for 72 h, after that, the viabilities and IC_{50} values of Caski and HUVEC cells were measured. As previously described, combination index (CI) was calculated to evaluate the synergistic effect of CSeD/SeD and TPP.

Furthermore, based on the interesting characteristics of Se element, e.g., metalloid properties, heavy metal effect, numerous studies have demonstrated that seleno compounds and Se nanomaterials have excellent radiosensitizer ability to improve the lethality of X-Ray.^{S1} Hence, we also evaluate the cytotoxicity against Caski and HUVEC cells induced by combined treatment of seleno compounds and different doses of X-Ray. As depicted previously, isobologram analysis was used to determine the interaction between seleno compounds and X-Ray.^{S2}

Hemolysis Analysis

Serial concentrations of compounds were mixed with red blood cells (RBCs) at 37 °C. Then, we measured the hemolysis rates and captured the pictures reflecting the morphology of RBCs at specific time intervals to assess the hemocompatibility, which would provide a basis for future clinical translation.

Colony Formation Assay

Caski and HUVEC cells were inoculated into six-well plates at a density of 2000 cells/well, respectively. After cell attachment, these cells were exposed to different

compounds (1.25 μM) and then cultured for another 10 days. For the SeD/CSeD groups initiated by TPP, the cells pre-cultured with TPP for 4 h were mixed with SeD/CSeD compounds. Finally, these cells were washed by PBS and fixed by paraformaldehyde, followed by stained with 0.5% crystal violet (wt/vol) and captured by optical camera.

Inhibitory Effects to Caski multicellular tumor spheroids

Caski multicellular tumor spheroids were formed by culturing Caski cells in an ultra low adsorption 6-well plate for 6 days. Then, the Caski spheroids were exposed to different concentrations of TPP-CSeD for 6 days and the relative volume changes ratio were calculated to evaluate the inhibitory effect on spheroid growth.

Transwell invasion assay

HUVEC cells growing in the logarithmic phase were added to the upper chamber covered with matrix glue. However, the inferior chamber was covered with 5% FBS medium (500 μL) with/without VEGF (50 ng/mL). Meanwhile, different compounds at a concentration of 1.25 μM were added to upper and inferior chambers. After 24 h of incubation, we used 0.1% crystal violet staining to invade cells fixed by paraformaldehyde under the surface of membrane and imaged with an inverted microscope. Manual counting was used for statistical analysis, and the inhibition rate was evaluated by setting inhibition rate of control cells was 100%.

***In vitro* cell migration and tube formation assay**

The effect of TPP-CSeD suppression on angiogenesis was detected by HUVEC cell migration assay and angiogenesis assay. A total of 4.0×10^5 HUVEC cells were inoculated and allowed to adhere for 24 h in 6-well plates. Then, scratches were created by using a sterile pipette tip (10 μL). Next, the cells were washed by PBS for three times and then cultured in 5% DMEM medium containing different compounds (1.25 μM) with or without VEGF (50 ng/mL) for 48 h. To obviously observe the wound-healing ability, we acquired the fluorescence images of cells which were

labeled with nucleus (green, Hoechst 33342) at 0 h, 24 h and 48 h of incubation.

The tube formation assay was performed as our described earlier. In brief, cells with a density of 5×10^4 cells/mL (1 mL) growing in the logarithmic phase were inoculated in 48-well plates, and then the medium containing different compounds were added to the cells and cultured for 6 h. The tube length of HUVEC cells was observed and photographed under microscope and then quantified by Image-J software.^{S3}

Flow cytometry analysis for mechanism of cell death induced by compounds and X-Ray

The mechanism of cell death induced by compounds and X-Ray was detected. Previous reported that cell arrest and apoptosis are the mainly pathway to induce cell death. Firstly, after different treatments for 24 h, we detected the Caski and HUVEC cells cycle distributions by flow cytometry according to previously described. On the other hand, Annexin V-FITC/PI double-staining kit (Beyotime, China) was introduced for apoptosis detection caused by compounds and X-Ray according to the manufacturer's instructions.

Mitochondrial morphography analysis

Crucially, as the driving force of cancer cells, mitochondria are responsible for generating available energy. Thus their rupture can be used as a strategy to observe cancer cell apoptosis. Hence, we used Mitotracker (green) and Hoechst (33342) probes to label mitochondria and nucleus of cells for detecting the mitochondrial fragmentation. Cells in confocal culture dish (2-cm) were incubated with TPP-CSeD and then irradiated with X-Ray (4 Gy). After incubating for 24 h, the cells were washed by PBS for three times and stained by Mitotracker for 2 h and then stained with Hoechst 33342 for 15 min. Finally, images were obtained using an Eclipse fluorescent microscope (Life Technologies) with a $\times 100$ oil immersion objective.

Caspase Activity Assay

Firstly, we extracted the proteins of Caski and HUVEC cells treated with X-Ray or combined with TPP-CSeD and X-Ray (4Gy). Next, we determined the protein concentrations in the cell lysates by bicinchoninic acid (BCA) method. Finally, the activities of caspase-3, caspase-8 and caspase-9 in the cell lysates were monitored by fluorometric method using Caspase Activity kit (Beyotime Institute of Biotechnology).^{S4}

Western Blotting Analysis

Western blotting was used to detect the expression levels of apoptosis signal pathway related proteins PARP and caspases-3/8/9 in Caski cells after different concentrations of TPP-CSeD combined with X-ray irradiation.

Statistical Analysis

All the experiments in this study were in triplicate. Data were expressed as mean \pm standard deviation (SD). Statistical analysis was carried out using the SPSS statistical package (version 18.0 for Windows; SPSS, Chicago, IL). Differences with $P < 0.05$ (*) or $P < 0.01$ (**) or $P < 0.001$ (***) were deemed statistically significant.

Result Section

Table S1 Cytotoxic effect of various compounds on cancer and normal cells with or without TPP initiating.

Compounds	IC ₅₀ (μM) ^a									
	Caski	HeLa	Siha	MCF-7	M231	HUVEC	E6/E7*	WI38*	SI ^b	SI ^b
TPP	91.28	162.75	177.3	236.90	57.97	319	282.35	69.33	3.09	0.75
CA-4	18.57	79.19	40.96	30	30.65	5.20	144.73	12.16	7.83	0.65
SeD	73.65	95.75	134.4	154.73	52.15	444.54	154.73	116.71	2.10	1.58
TPP-SeD	52.09	53.67	60.37	71.92	17.79	175.20	71.92	46.37	1.38	0.89
CSeD	6.88	30.05	57.29	43.19	18.71	2.86	43.19	52.245	6.27	7.59
TPP-CSeD	1.38	12.83	34.15	22.31	7.02	1.72	22.31	27.11	16.16	19.64

a Treatment time: 72 h

b SI = IC₅₀(E6/E7)/IC₅₀(Caski), SI=IC₅₀(Wi38)/IC₅₀(Caski)

* Normal cells.

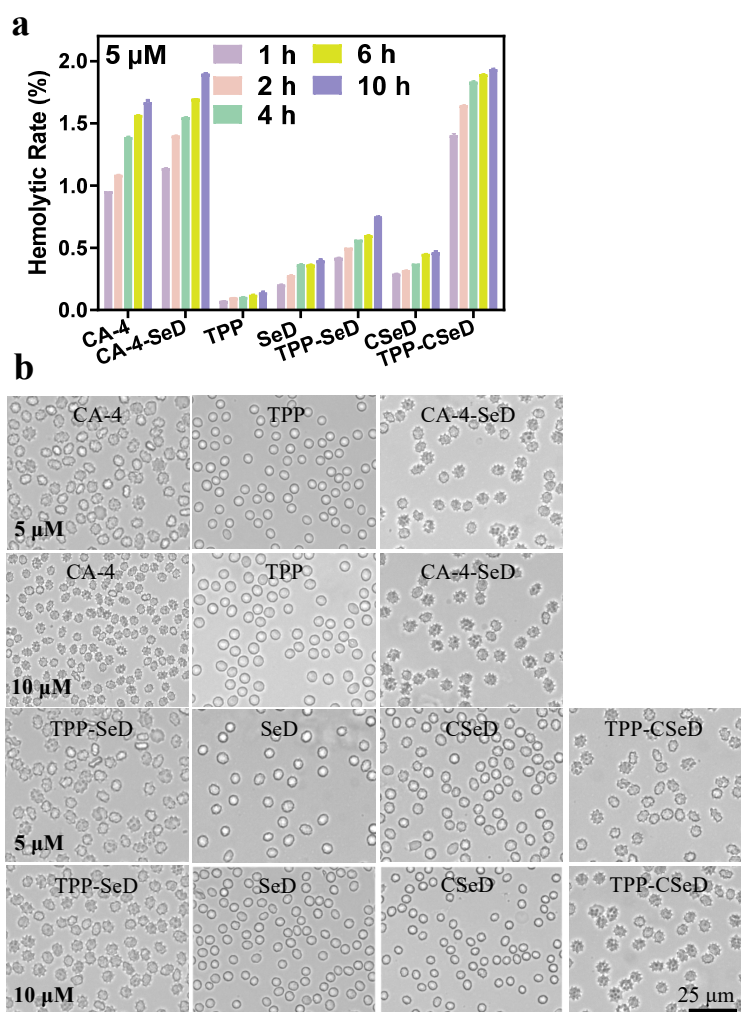


Fig. S1 (a) Effects of different compounds with concentration of 5 μM on hemolysis of RBCs. **(b)** Representative photographs of RBCs after incubated with different compounds in concentrations of 5 μM or 10 μM for 10 h.

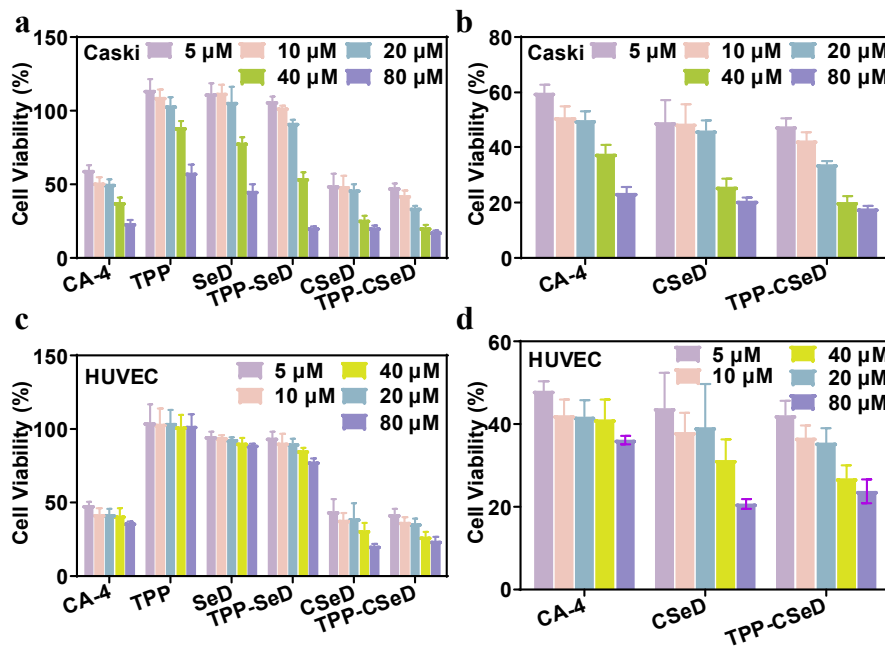


Fig. S2 Antiproliferative effect of compounds with different concentrations against Caski (a) and HUVEC (c) cells for 72 h of incubation. (b) (d) Magnification certain parts of (a) and (c).

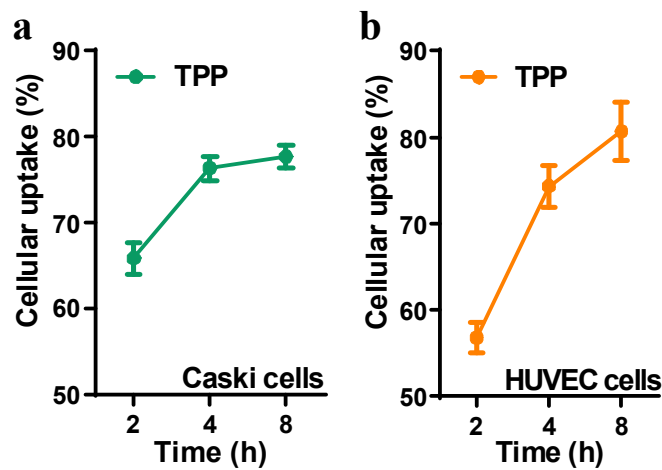


Fig. S3 Cellular uptake efficiency of TPP in Caski (a) and HUVEC (b) cells incubated for 2 h, 4 h and 8 h, respectively, as detected by ICP-MS.

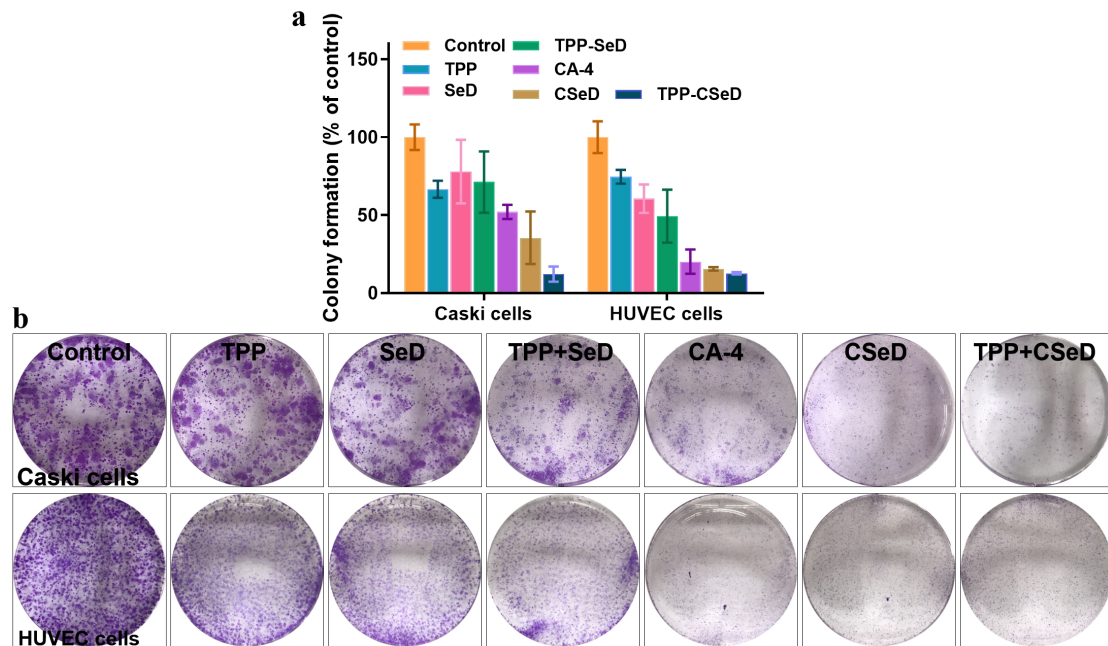


Fig. S4 Compounds suppress colony formation of Caski and HUVEC cells. (a) Quantitative of different compounds suppress the colony formation of Caski and HUVEC cells. **(b)** Representative graphs of colony formation of Caski and HUVEC cells exposed to different compounds.

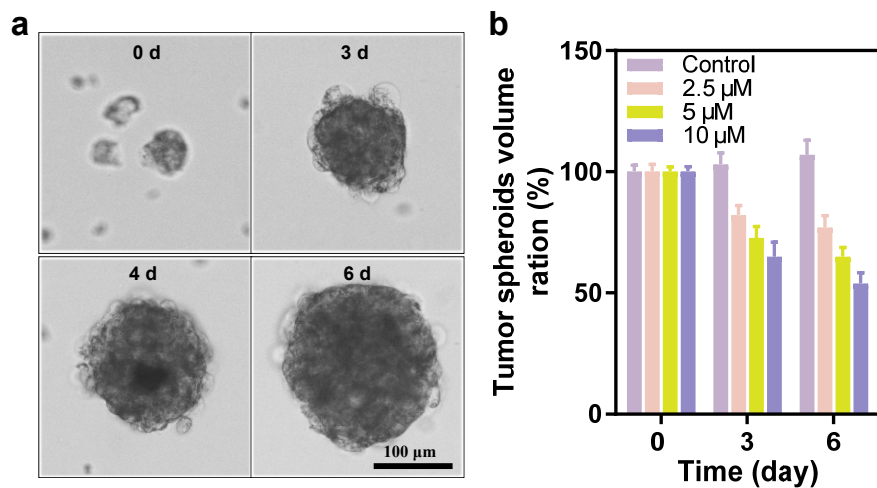


Fig. S5 TPP-CSeD inhibit the growth of Caski spheroids. (a) Formation process of Caski tumor spheroids within 6 days. **(b)** Quantitative of the growth Inhibition of TPP-CSeD for Caski spheroids.

Table S2 IC₅₀ values of CA-4 and seleno compounds with or without TPP initiating to Caski and HUVEC cells in combination of X-Ray with different dosages.

Complex	IC ₅₀ (μM) (Caski cells)				Complex	IC ₅₀ (μM) (HUVEC cells)			
	0 Gy	2 Gy	4 Gy	8 Gy		0 Gy	2 Gy	4 Gy	8 Gy
CA-4	18.57	17.09	16.22	14.35	CA-4	5.20	5.03	4.21	2.40
SeD	73.65	63.24	55.98	45.48	SeD	444.54	221.4	158.33	63.99
TPP-SeD	52.09	43.32	36.80	29.37	TPP-SeD	175.20	120.32	94.35	36.421
CSeD	6.66	4.19	3.47	2.9	CSeD	2.86	2.18	1.62	0.65
TPP-CSeD	1.38	1.00	0.78	0.61	TPP-CSeD	1.724	1.31	0.88	0.41

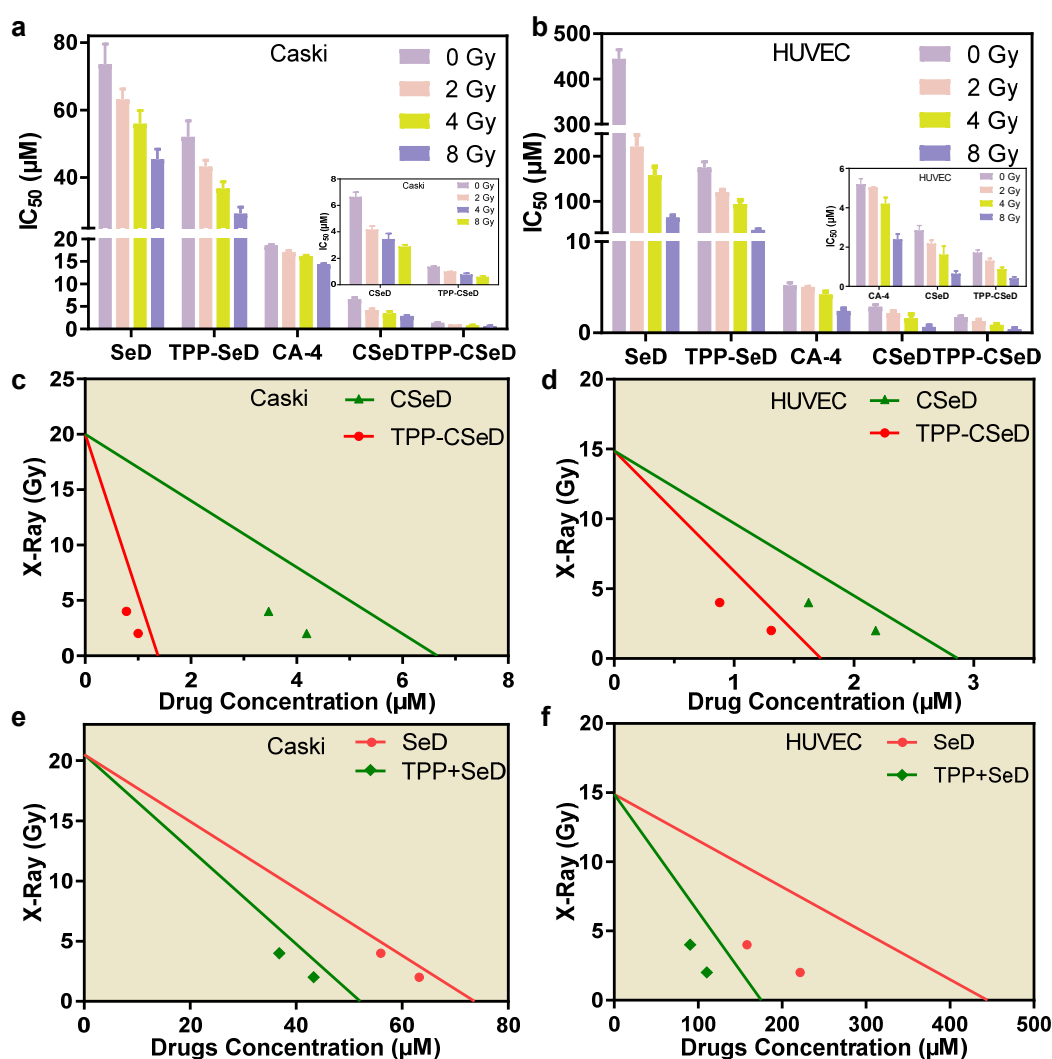


Fig. S6 Anticancer efficiency of different compounds with X-Ray irradiation. (a-b) Growth inhibition of compounds combined with radiation treatment on Caski and HUVEC cells. (c-f) Isobologram analysis indicates the synergistic relationship of seleno compounds and X-Ray in Caski and HUVEC cells.

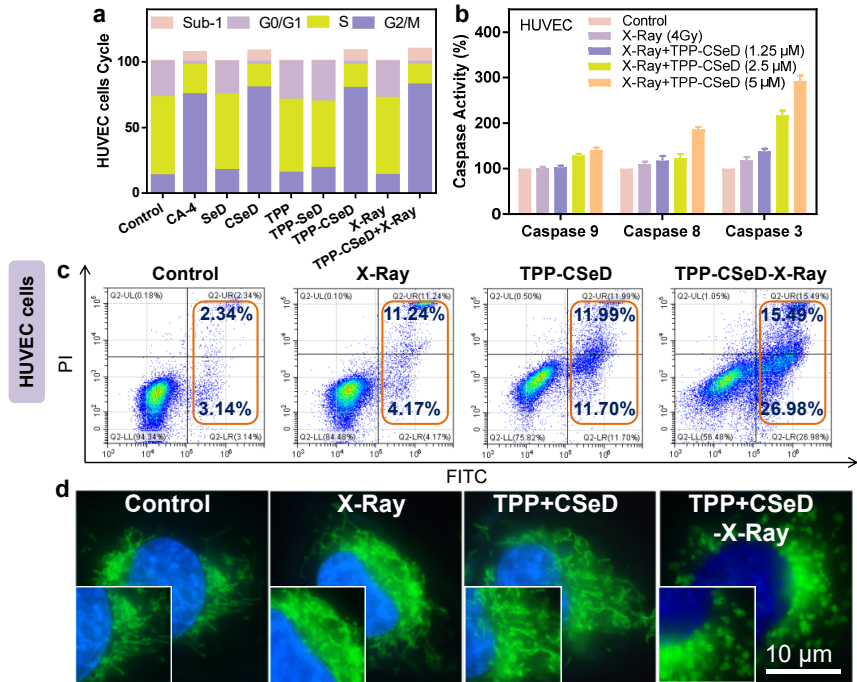


Fig. S7 Action mechanisms of cell death induced by compounds and X-ray radiotherapy for HUVEC cells. **(a)** Cell cycle distribution of HUVEC cells caused by different treatments for 24 h. **(b)** Combined treatments of X-Ray and compounds activated caspase3/8/9 activity in HUVEC cells. **(c)** Apoptosis proportion of the HUVEC cells after different treatments. **(d)** Representative images of mitochondrial fragmentation in HUVEC cells after incubation with TPP-CSeD and irradiation with X-Ray.

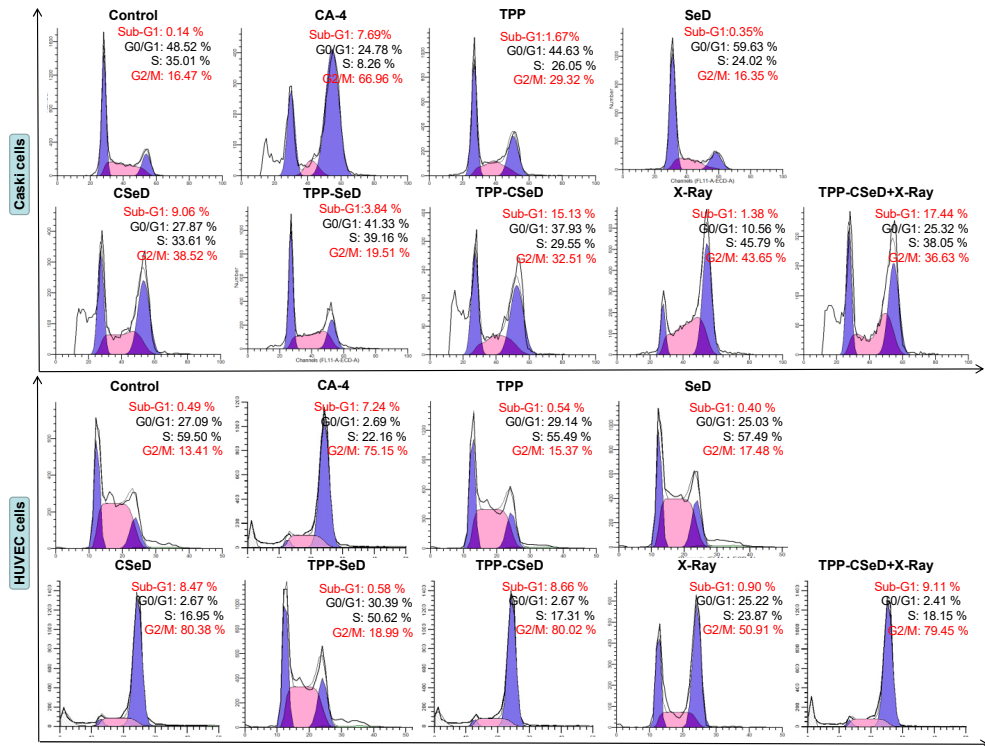


Fig. S8 Flow cytometric analysis of Caski and HUVEC cell treated with different compounds for 24 h.

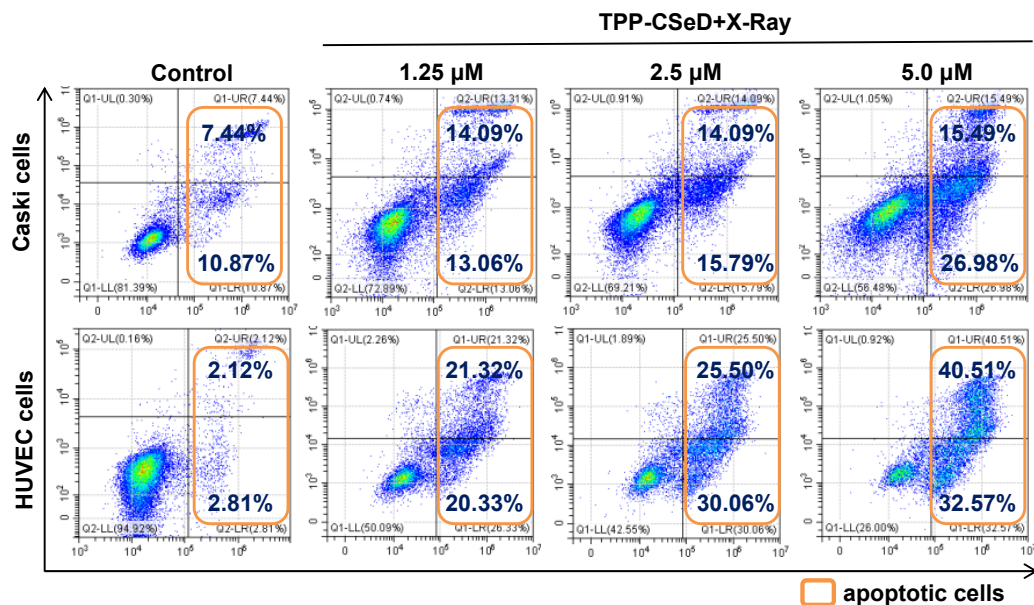


Fig. S9 Flow cytometric analysis of apoptosis proportion induced by different concentrations of TPP-CSeD combined with X-Ray in Caski and HUVEC cells.

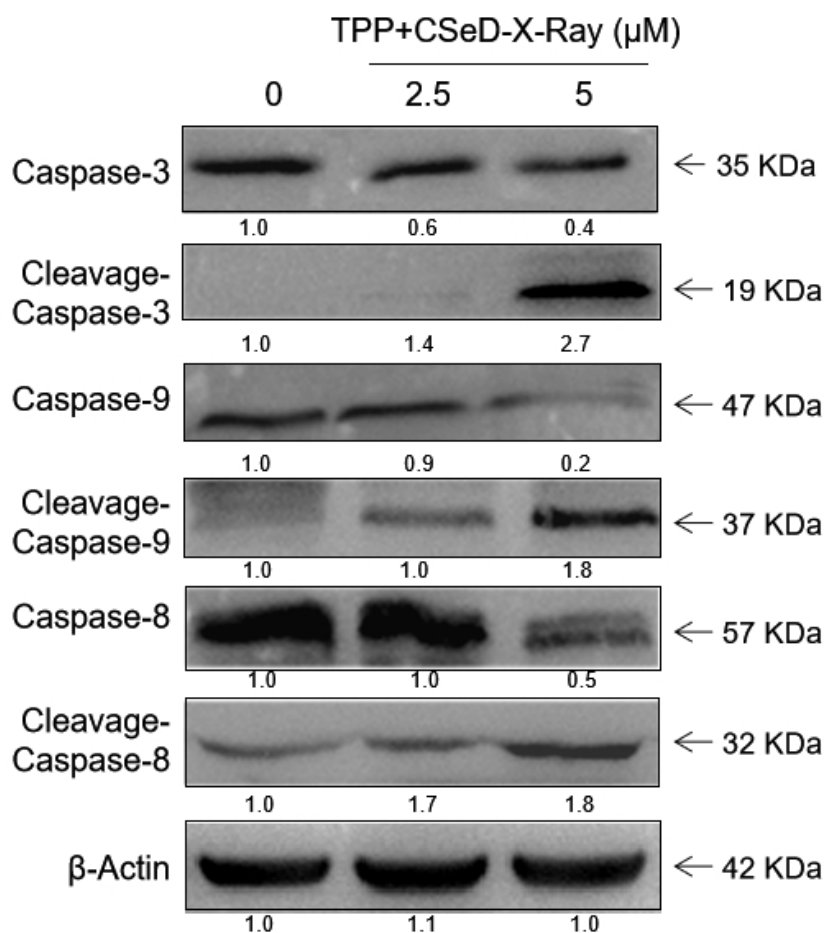
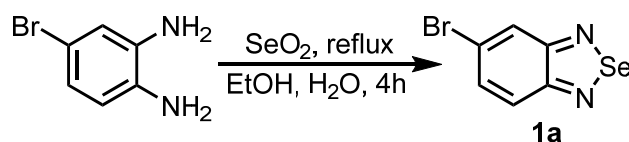


Fig. S10 Effects of different concentrations of TPP-CSeD and X-Ray on the expression levels of caspase family members in Caski cells by western blot analysis. The variations of protein expression levels were shown as ratios of each group.

Chemistry experiments section

All commercially available reagents were used as received. Analytical grade solvents were bought and without further purification. The reactions were carried out under mild environment, magnetically stirred, and monitored by thin layer chromatography (TLC), visualized by fluorescence quenching under UV light (Otherwise noted). NMR spectra were recorded on a Bruker Ascend 300 spectrometer operating at 300 MHz for ^1H acquisitions, 75 MHz for ^{13}C acquisitions and ^{31}P acquisitions or Bruker Ascend 400 spectrometer operating at 400 MHz for ^1H acquisitions, 101 MHz for ^{13}C acquisitions and ^{31}P acquisitions. Chemical shifts were referenced to the residual proton solvent peaks solvent ^1H signals (CDCl_3 , 7.26; $(\text{CD}_3)_2\text{SO}$, 2.50), solvent ^{13}C signals (CDCl_3 , 77.16; $(\text{CD}_3)_2\text{SO}$, 39.60). Signals are listed in ppm, and multiplicity identified as s = singlet, br = broad, d = doublet, t = triplet, q = quartet, m = multiplet; coupling constants in Hz; integration. High-resolution mass spectra were obtained using Agilent LC-UV-TOF mass spectrometer and TripleTOF™ 5600+ mass spectrometer. Yields refer to spectroscopically pure compounds.

Synthetic section of various compounds



Briefly, in the 500 mL round-bottom flask, the solution of selenium dioxide 4.45 g (40.1 mmol, 1.5eq) in 15 mL H_2O was slowly added to the solution of phenylenediamines 5 g (26.73 mmol, 1eq) in 150 mL ethanol. The mixture was stirred and refluxed for 4 h. When the reaction finished, the mixture was concentrated under reduced pressure, then extracted by EtOAc (EA). The crude product was purified by chromatography on silica gel, eluting with Petroleum ether (PE) : EtOAc (EA) = 10:1 (v/v) to afford the pure product as white solid (6.58 g, yield = 94%). The reaction was monitored by TLC plate.

NMR Spectroscopy: ^1H NMR (400 MHz, CDCl_3 , 25 °C, δ): 8.07 (s, 1H), 7.70 (d, *J*

= 9.36Hz, 1H), 7.54 (d, $J = 9.4$ Hz, 1H). ^{13}C NMR (101 MHz, CDCl_3 , 25 °C, δ): 160.67, 158.99, 133.32, 125.47, 123.84.

Mass Spectrometry: HRMS (ESI-TOF) (m/z): calcd for $\text{C}_6\text{H}_4\text{BrN}_2\text{Se}^+$ ($[\text{M}+\text{H}]^+$), 262.8718, found, 262.8713.

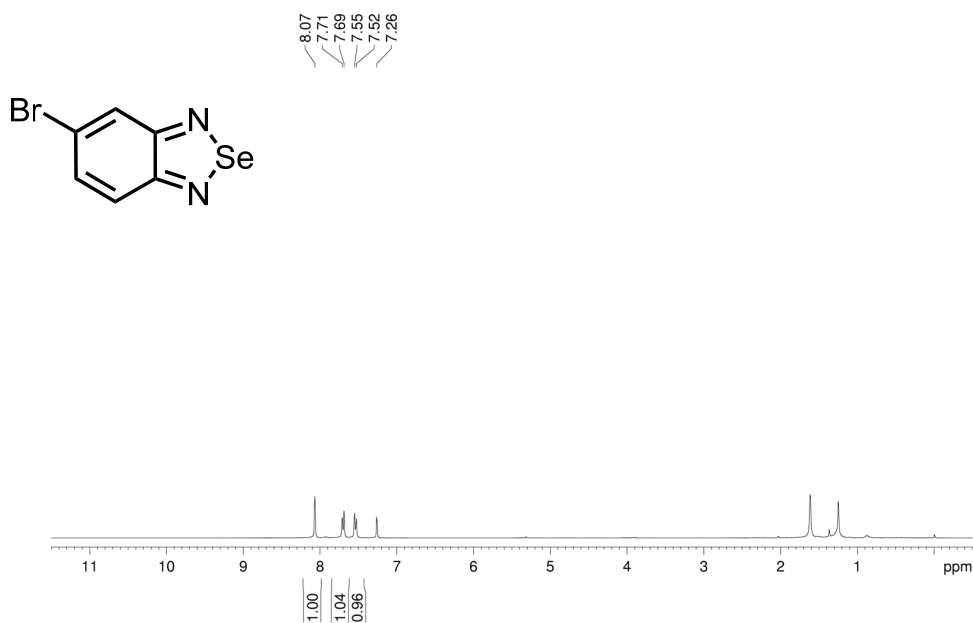


Fig. S11 ^1H NMR (400 MHz, CDCl_3 , 297 K) spectrum of 1a.

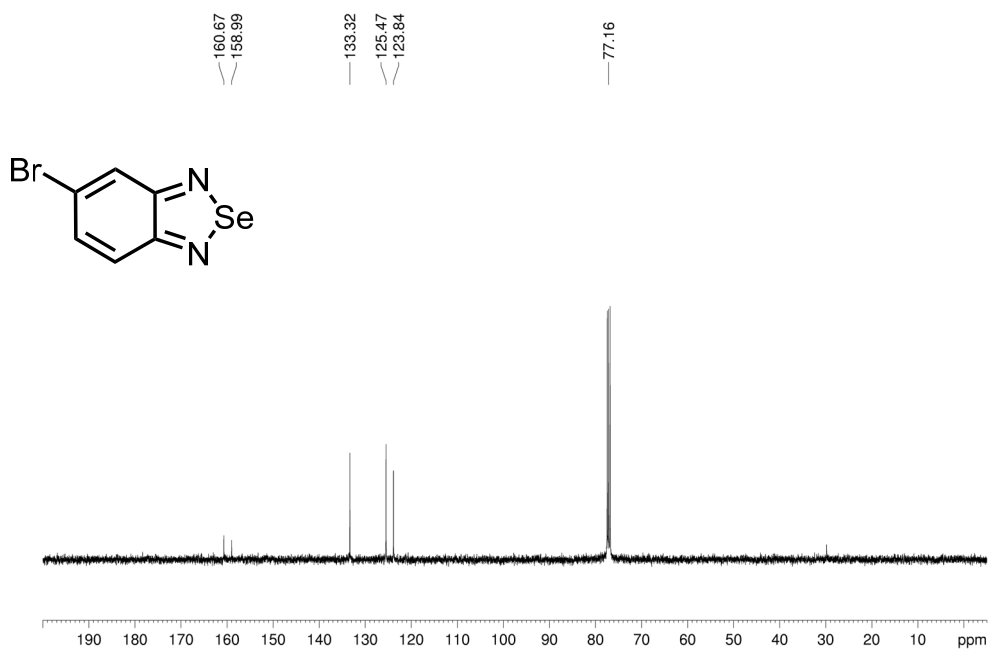
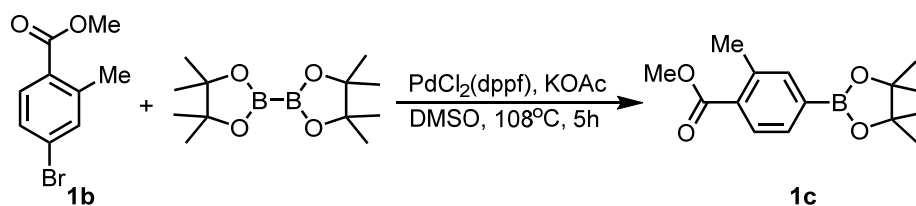


Fig. S12 ^{13}C NMR (101 MHz, CDCl_3 , 297 K) spectrum of 1a.



In the 250 mL schlenk bottle, 1b (1 g, 4.37 mmol, 1 eq), pinacol (1.66 g, 6.55 mmol, 1.5 eq), KOAc (0.86 g, 8.73 mmol, 2 eq), PdCl₂(dppf) (0.32 g, 0.44 mmol, 0.1 eq), were dissolved in 60 mL DMSO under N₂ atmosphere, the reaction was heated to 108°C lasted for 5 h. The mixture was partitioned between EtOAc (30 mL) and H₂O (150 mL) for 3 times, the aqueous was extracted by EtOAc (30 mL × 3). The combined organic phase was dried over MgSO₄, concentrated in vacuo. The crude product was purified by chromatography on silica gel, eluting with PE : EA = 15:1 (v/v), to afford the light yellow oil as product 1c (0.64 g, yield = 53%).

NMR Spectroscopy: ¹H NMR (300 MHz, DMSO, 25 °C, δ): 7.78 (d, *J* = 7.62 Hz, 1H), 7.58 (d, *J* = 10.35 Hz, 2H), 3.77 (s, 3H), 1.24(s, 12H). ¹³C NMR (75 MHz, CDCl₃, 25 °C, δ): 167.93, 138.92, 137.91, 131.87, 131.78, 129.56, 84.01, 51.75, 24.81, 21.41.

Mass Spectrometry: HRMS (ESI-TOF) (*m/z*): calcd for C₁₅H₂₂BO₄⁺ ([M+H])⁺, 277.1606, found, 277.1614.

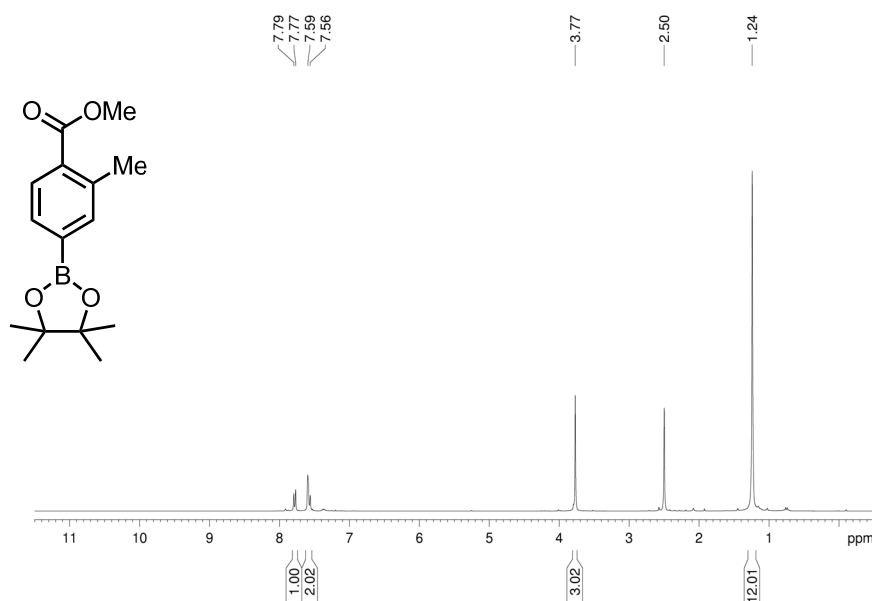


Fig. S13 ¹H NMR (300 MHz, DMSO-d₆, 297 K) spectrum of 1c.

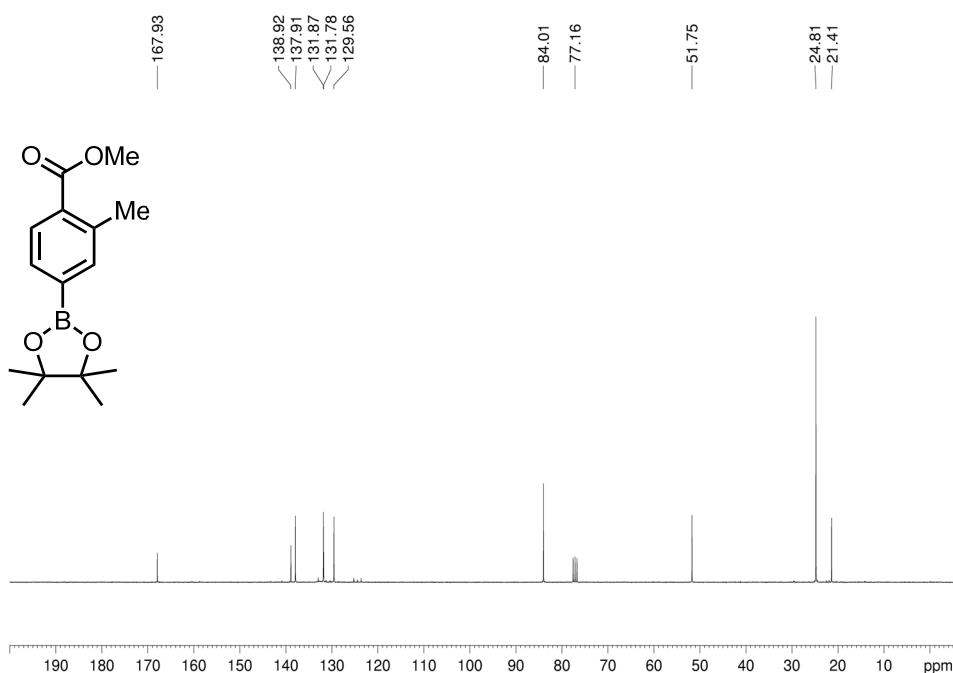
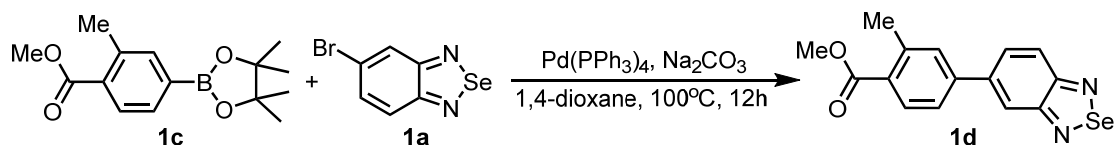


Fig. S14 ^{13}C NMR (75 MHz, DMSO- d_6 , 297 K) spectrum of 1c.



Reactant 1c (0.5 g, 1.81 mmol, 1 eq), 1a (0.95 g, 3.62 mmol, 2 eq), Pd(PPh₃)₄ (0.2 g, 0.18 mmol, 0.1 eq) were dissolved in 1,4-dioxane 80 mL under N₂ atmosphere in 250 mL schlenk bottle. Na₂CO₃ (0.38 g, 3.62 mmol, 2 eq) was dissolved in 2 mL ultra-pure water and injected into the system. The reaction was heated to 100 °C and lasted for 12 h. After reaction completed, the mixture was partitioned between DCM (30 mL) and H₂O (120 mL) 3 times. The aqueous was extracted by DCM (30 mL × 3). The organic phase was combined and dried over MgSO₄, evaporated under reduced pressure and purified by column chromatography on silica gel with PE : EA = 10:1-5:1 (v/v) as eluent to afford yellow solid corresponding product 1d (0.23 g, yield = 38.7%).

NMR Spectroscopy: ^1H NMR (300 MHz, CDCl₃, 25 °C, δ): 8.05 (d, J = 7.89 Hz, 2H), 7.91 (d, J = 9.33 Hz, 1H), 7.78 (d, J = 9.33 Hz, 1H), 7.58 (d, J = 6.57 Hz, 2H). 3.93 (s, 3H), 2.71 (s, 3H). ^{13}C NMR (75 MHz, CDCl₃, 25 °C, δ): 167.78, 142.74,

141.26, 141.23, 131.62, 130.68, 130.09, 129.50, 124.69, 123.67, 120.89, 52.11, 22.15.

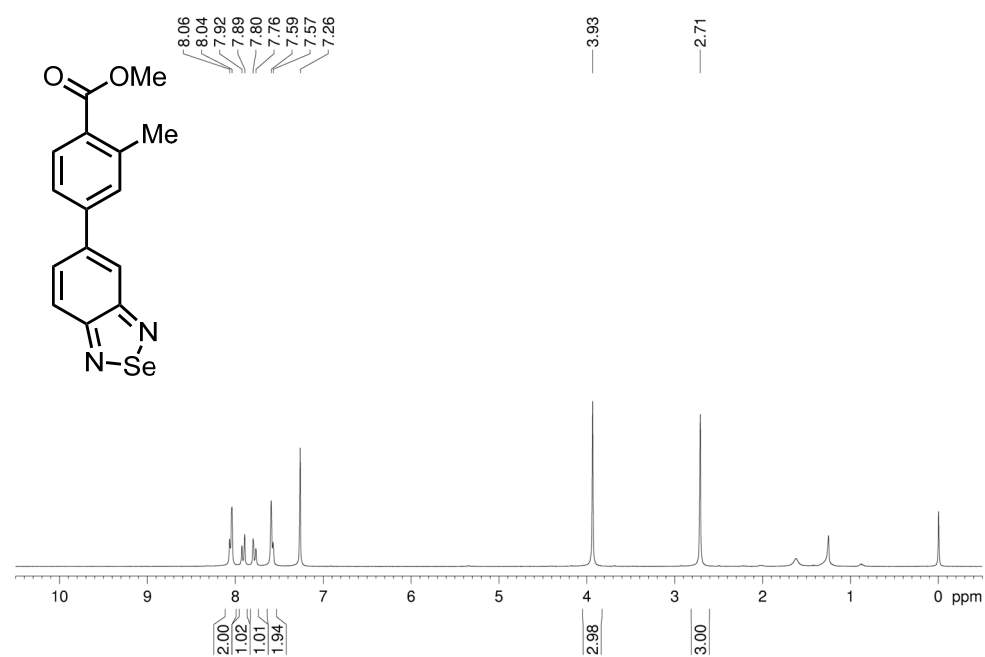


Fig. S15 ¹H NMR (300 MHz, CDCl₃, 297 K) spectrum of 1d.

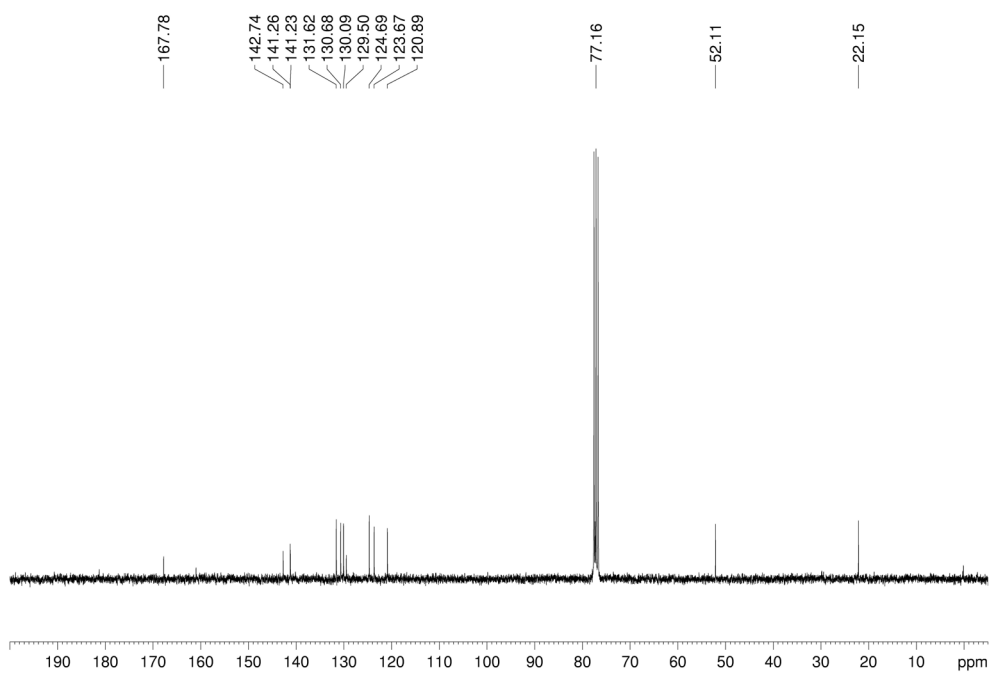
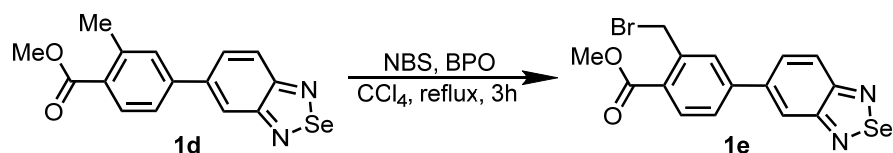


Fig. S16 ¹³C NMR (75 MHz, CDCl₃, 297 K) spectrum of 1d.



A mixture of 1d (0.3 g, 0.91 mmol, 1 eq), NBS (0.24 g, 1.37 mmol, 1.5 eq), BPO (0.044 g, 0.18 mmol, 0.2 eq), was dissolved by CCl₄ 50 mL in the 100ml round bottom flask. The reaction was heated to reflux and stirred for 3 h. Afterward, the solvent would need to be removed by rotary evaporator under reduced pressure, the obtained residue was purified by column chromatography on silica gel with PE : EA=10:1 (v/v) as eluent to give the product as yellow solid (0.25 g, yield = 66.99%).

NMR Spectroscopy: ¹H NMR (300 MHz, CDCl₃, 25 °C, δ): 8.11 (d, *J* = 8.22 Hz, 1H), 8.06 (s, 1H), 7.93 (d, *J* = 9.39 Hz, 1H), 7.81-7.76 (m, 2H), 7.70 (dd, *J* = 8.13 Hz, 1.5 Hz, 1H), 5.06 (s, 2H), 3.98 (s, 3H). ¹³C NMR (75 MHz, CDCl₃, 25 °C, δ): 166.75, 143.51, 140.38, 132.37, 130.66, 129.72, 128.76, 127.28, 123.92, 121.21, 52.60, 31.46.

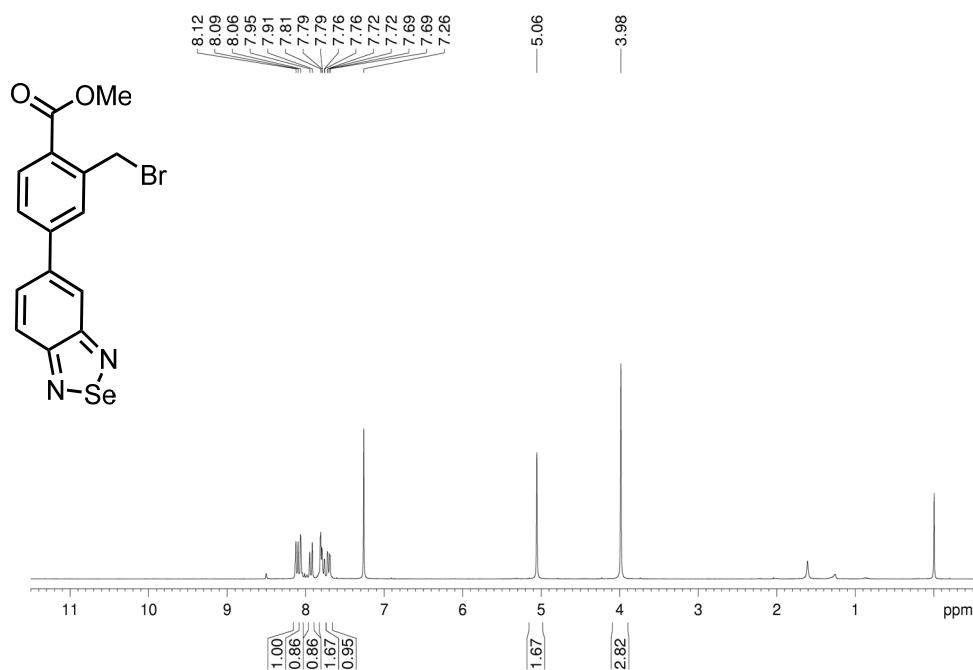


Fig. S17 ¹H NMR (300 MHz, CDCl₃, 297 K) spectrum of 1e.

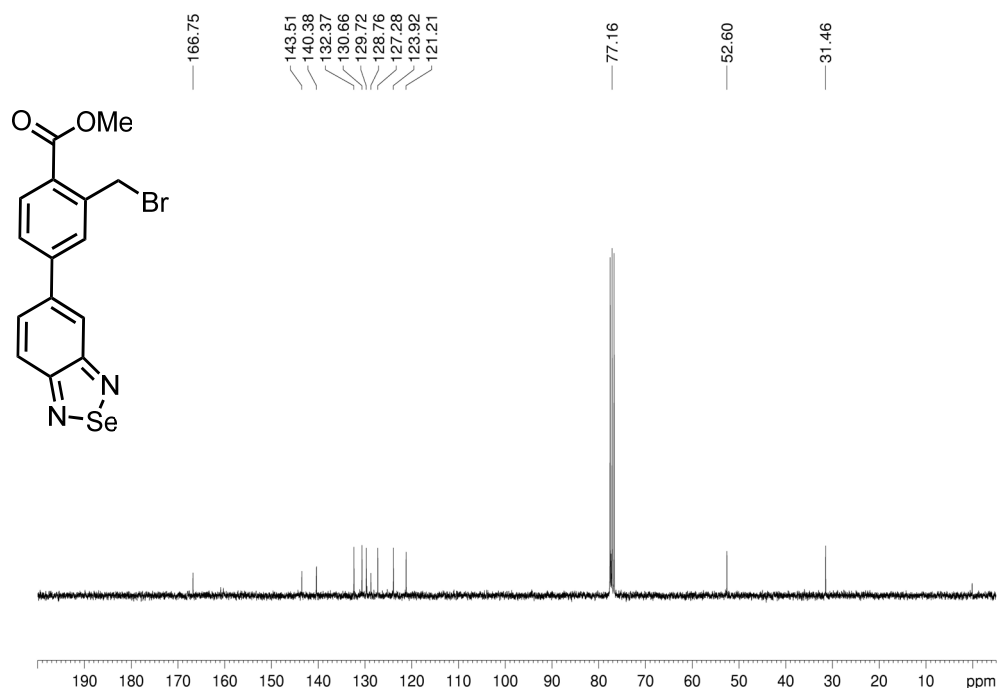
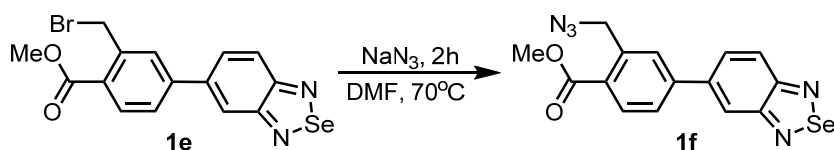


Fig. S18 ^{13}C NMR (75 MHz, CDCl_3 , 297 K) spectrum of **1e**.



The solution of **1e** (0.1 g, 0.3 mmol, 1 eq), NaN_3 (0.03 g, 1.5 mmol, 5 eq) in 30ml DMF was heated to 70 °C and lasted for 2 h. After this period, the mixture was partitioned between saturated lithium chlorid solution (50 mL) and EtOAc (30 mL). The combined organic phase was washed by saturated lithium chlorid solution (50 mL \times 3), and evaporated under reduced pressure. The residue was purified by column chromatography on silica gel with PE : EA = 10:1 (v/v), to afford light brown solid (0.11 g, yield = 98.50%).

NMR Spectroscopy: ^1H NMR (400 MHz, CDCl_3 , 25 °C, δ): 8.16 (d, J = 8.12 Hz, 1H), 8.08 (s, 1H), 7.94 (d, J = 9.32 Hz), 7.85 (s, 1H), 7.80 (d, J = 9.24 Hz, 1H), 7.74 (d, J = 8.12 Hz, 1H), 4.95 (s, 2H), 3.97 (s, 3H). ^{13}C NMR (101 MHz, CDCl_3 , 25 °C, δ): 166.89, 160.88, 160.24, 143.66, 140.67, 138.61, 132.20, 129.83, 128.47, 128.35, 126.82, 123.90, 121.24, 53.31, 52.54.

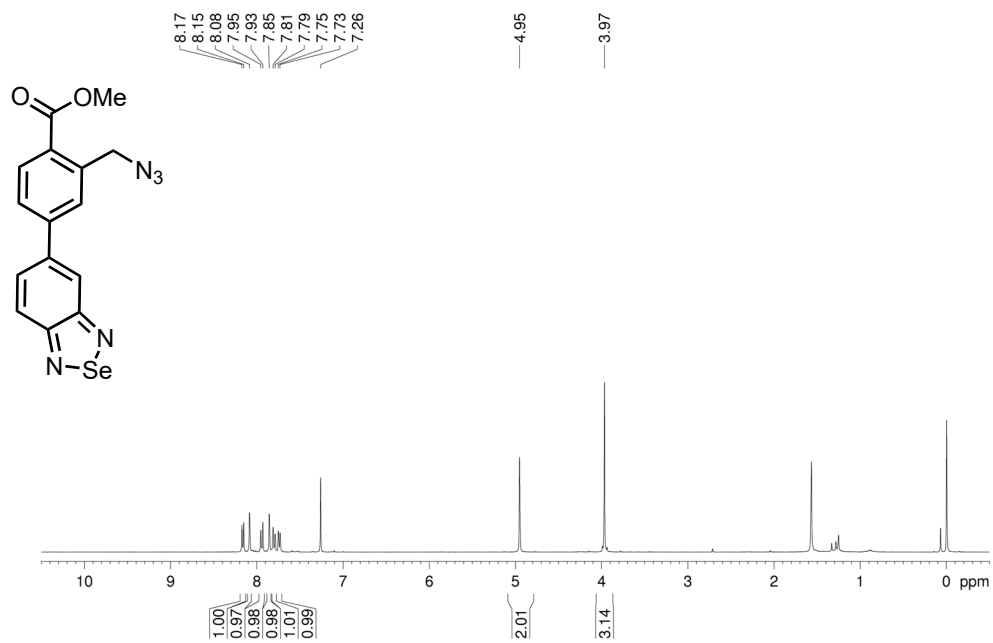


Fig. S19 ¹H NMR (400 MHz, CDCl₃, 297 K) spectrum of 1f.

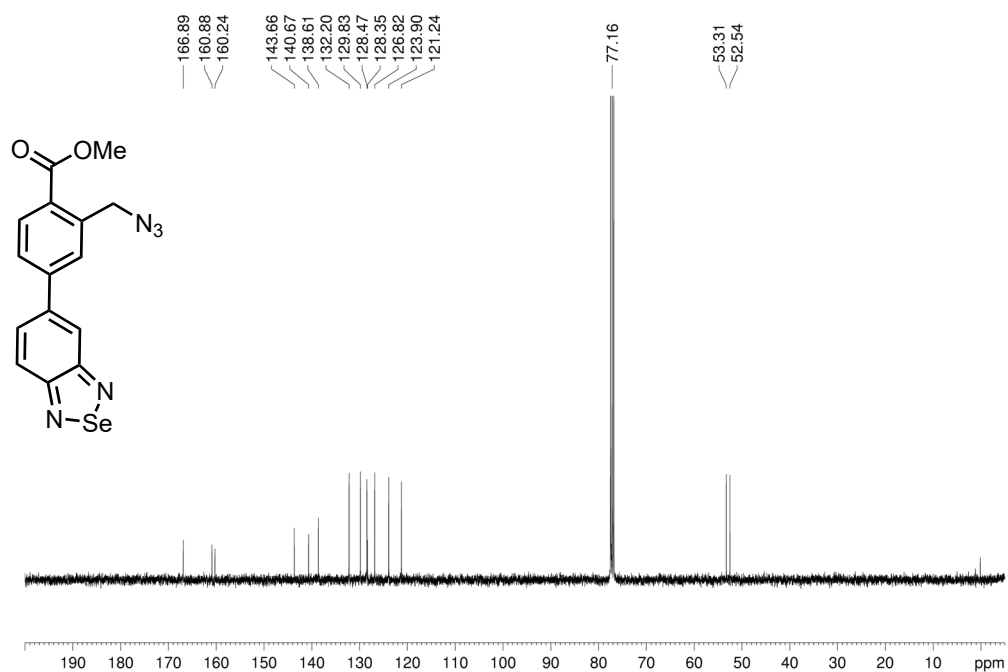
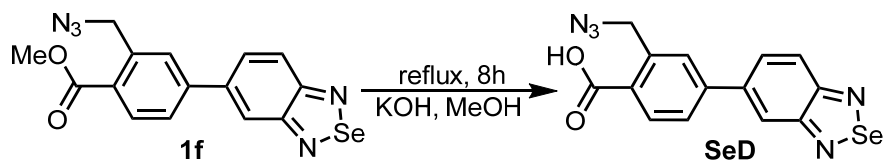


Fig. S20 ¹³C NMR (101 MHz, CDCl₃, 297 K) spectrum of 1f.



The mixture of reagent 1e (0.15 g, 0.40 mmol, 1eq) and KOH (0.023 g, 4 mmol, 10eq) was dissolved in MeOH (20 mL). The reaction was heated to reflux and stirred for 8h. After this progress, the solvent was evaporated under reduced pressure. The residue was dissolved by H₂O (20 mL) and adjusted the pH to < 6. The aqueous was extracted by DCM (50 mL × 3). The crude product was purified by column chromatography on silica gel with PE : EA = 2:1 (v/v), to afford brown solid (0.14 g, yield = 97.71%).

NMR Spectroscopy: ¹H NMR (400 MHz, DMSO, 25°C, δ): 8.24 (s, 1H), 8.09-8.06 (m, 2H), 8.00 (d, *J* = 7.8 Hz, 3H). ¹³C NMR (101 MHz, DMSO, 25 °C, δ): 167.73, 160.14, 159.47, 142.12, 139.15, 137.40, 131.81, 129.80, 129.51, 129.15, 127.11, 123.73, 120.67, 52.16.

Mass Spectrometry: HRMS (ESI-TOF) (*m/z*): calcd for C₁₄H₈N₅O₂Se⁻ ([M-H])⁻, 357.9849, found, 357.9856.

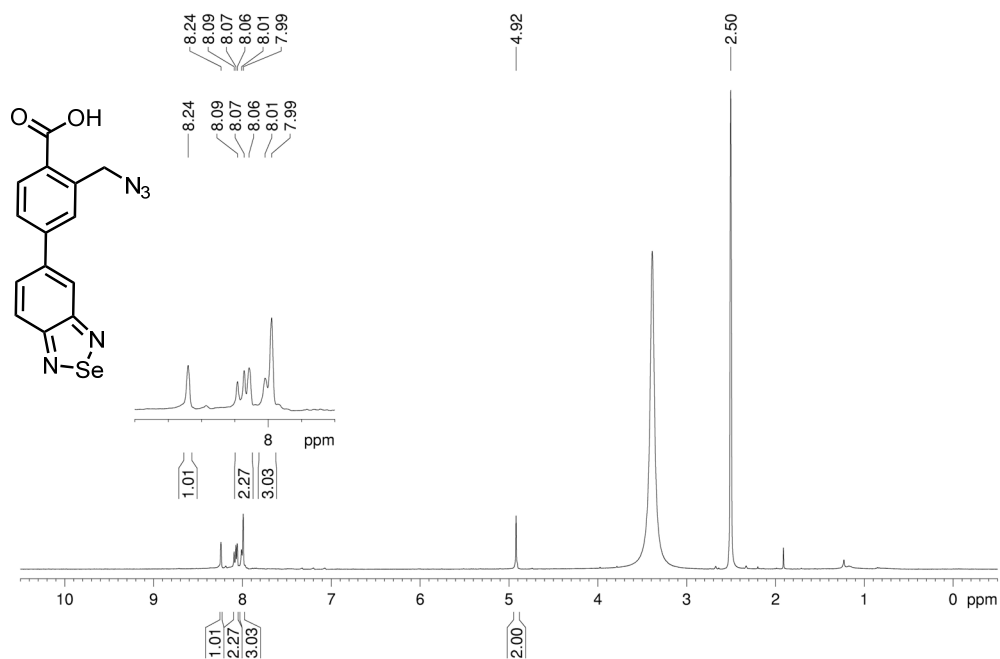


Fig. S21 ¹H NMR (400 MHz, CDCl₃, 297 K) spectrum of SeD.

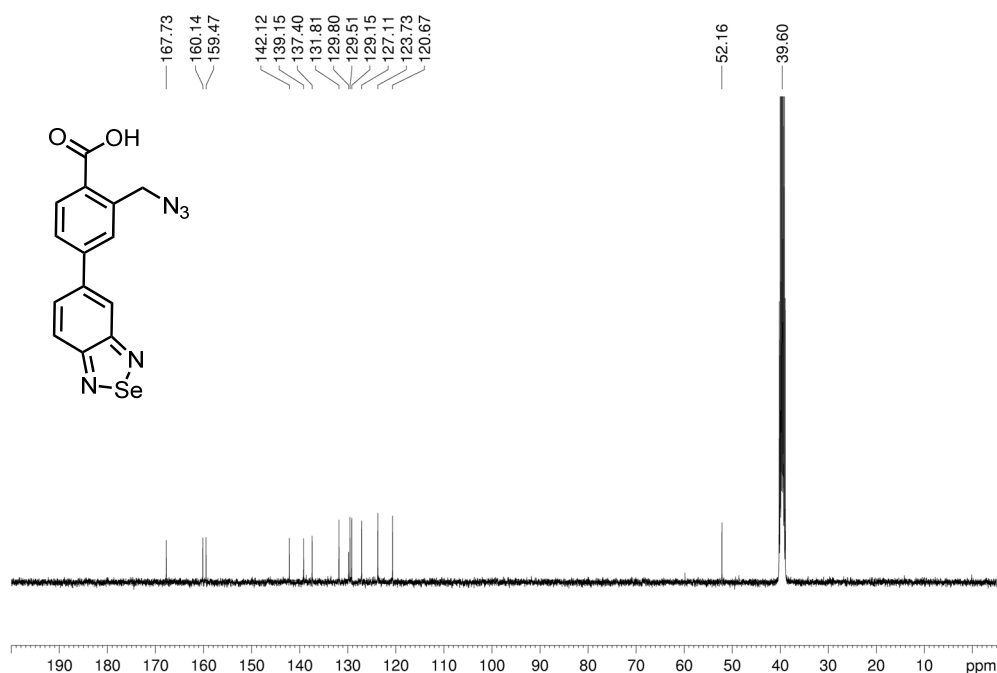
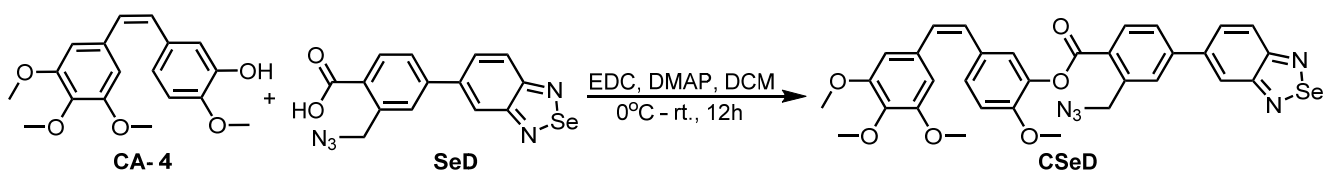


Fig. S22 ^{13}C NMR (101 MHz, $\text{DMSO-}d_6$, 297 K) spectrum of SeD.



The mixture of CA-4 (20 mg, 0.063 mmol, 1 eq), SeD (23 mg, 0.063 mmol, 1 eq), DMAP (6.23 mg, 0.051 mmol), DCM (2 mL, anhydrous) was stirred in the schlenk tube at 0°C for 0.5 h. After the solid was dissolved completely, EDC (14.57 mg, 0.076 mmol, 1.2 eq), was added into the system. The reaction was slowly heated to the room temperature and stirred for 12 h. The mixture was washed with H_2O (10 mL) and extracted with DCM (10 mL). After evaporated, the crude residue was purified by column chromatography on silica gel with PE : EA = 5:1 (v/v), to afford light yellow solid (22 mg, yield = 53.15%).

NMR Spectroscopy: ^1H NMR (400 MHz, CDCl_3 , 25°C , δ): 8.42 (d, $J = 8.12$ Hz, 1H), 8.13(s, 1H), 7.97 (d, $J = 10\text{Hz}$, 2H), 8.00 (d, 2H), 7.83 (dd, $J = 7.52$ Hz, 5.76 Hz, 2H), 7.39 (d, $J = 8.44$ Hz, 2H), 7.03 (d, $J = 8.2$ Hz, 1H), 6.95 (d, $J = 4.8$ Hz, 2H), 6.72 (s, 2H), 5.03 (s, 2H), 3.91(s, 6H), 3.87 (d, $J = 6.08$ Hz 6H). ^{13}C NMR (101 MHz,

CDCl₃, 25 °C, δ): 164.56, 160.88, 160.28, 153.54, 150.79, 144.32, 140.64, 139.99, 139.39, 137.98, 133.20, 132.82, 130.89, 129.80, 128.42, 127.92, 127.47, 127.00, 126.93, 125.78, 123.99, 121.39, 120.51, 112.66, 103.56, 61.12, 56.25, 56.20, 53.17, 29.84.

Mass Spectrometry: HRMS (ESI-TOF) (m/z): calcd for C₃₂H₂₇N₅NaO₆Se⁺, ([M + Na]⁺, 680.1028, found, 680.1032.

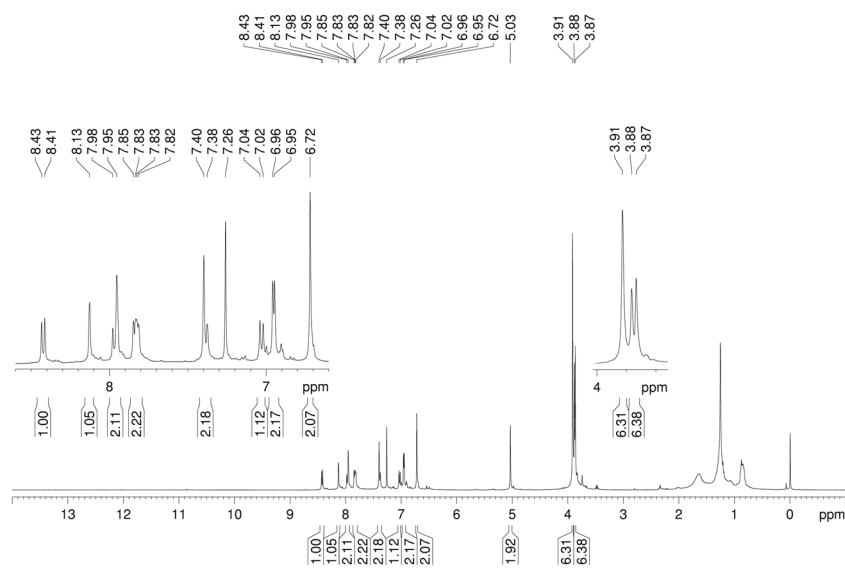


Fig. S23 ¹H NMR (400 MHz, CDCl₃, 297 K) spectrum of CSeD.

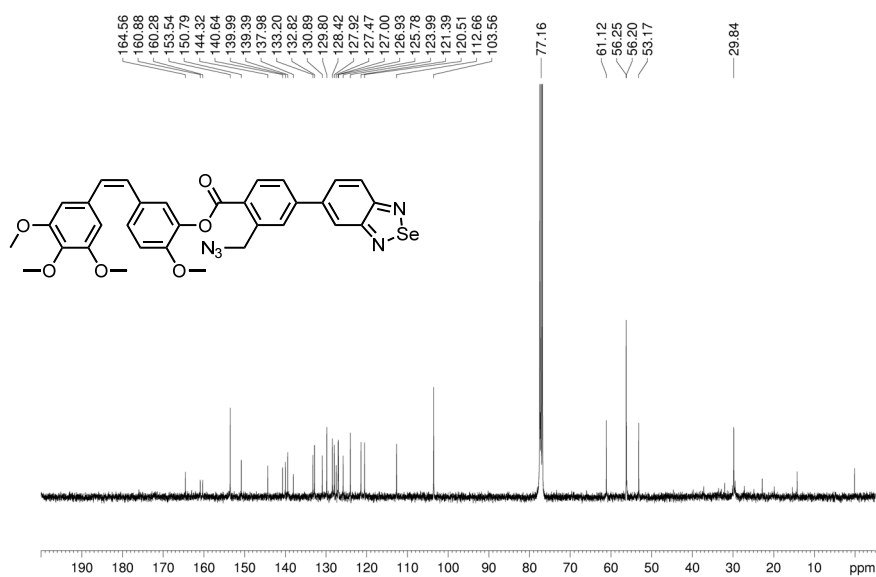


Fig. S24 ¹³C NMR (101 MHz, CDCl₃, 297 K) spectrum of CSeD.

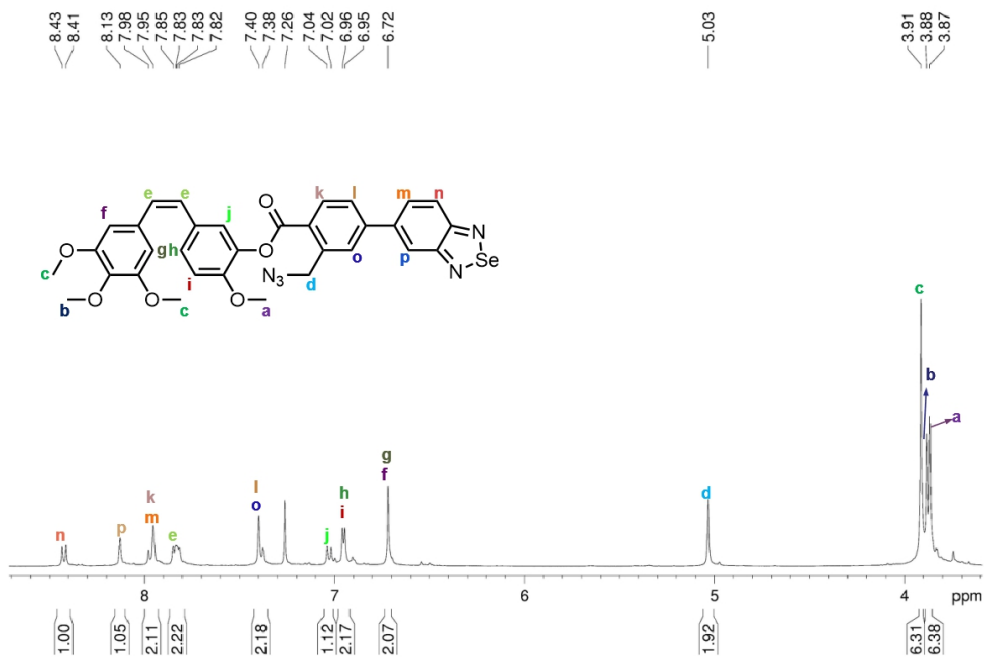


Fig. S25 Assignment of proton peaks of CSeD

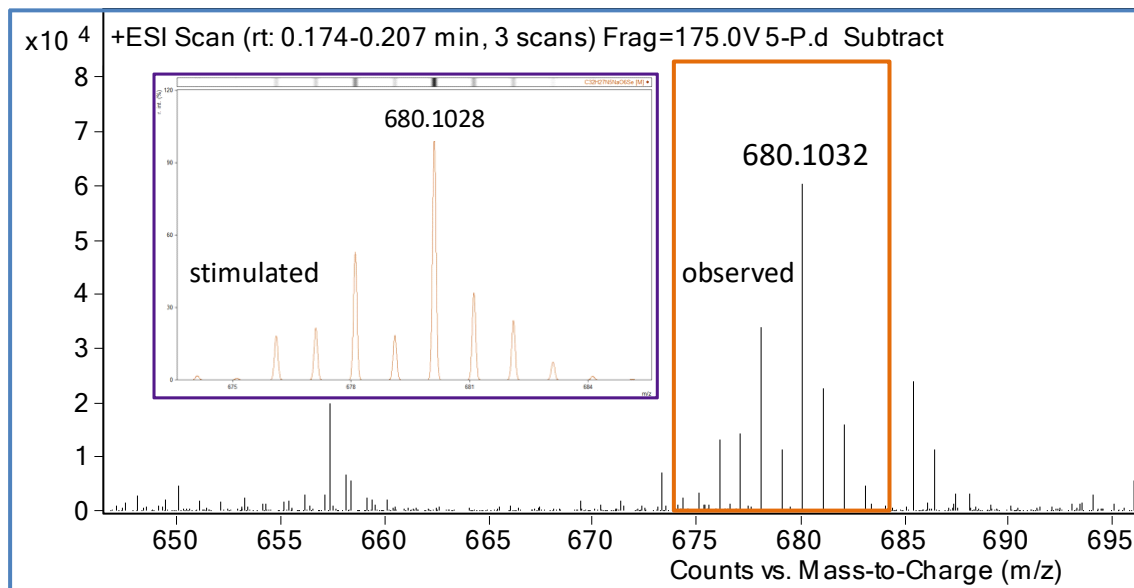


Fig. S26 ESI-MS of CSeD

The monitoring of the procedure of TPP initiating CSeD *in vitro in* different ways

1, ^1H NMR monitoring the TPP initiates CSeD staudinger reaction

The mixture of CSeD (1.0 eq) and TPP (1.0 eq) was dissolved by CDCl_3-d (0.5 mL) in NMR tube. The ^1H NMR detection on the solvent was performed immediately, after that the detection was performed every 15 minutes and lasted for 4 h.

2, ^{31}P NMR monitoring the TPP changed to TPO

After initiated the mixture of CSeD and TPP in PBS solution for 4 h, the ^{31}P NMR detection on the mixture was performed and compared with the ^{31}P NMR of reagent TPP.^{S5}

3, HMRS observation of

The solution of CSeD (8 mg, 1.0 eq) in DMSO was combined with the solution of TPP (2.6 mg, 2.0 eq) in PBS with the portion of $v : v=1:1$. After that, the combined mixture was stirred in room temperature for 4 h and performed HRMS detection.^{S6}

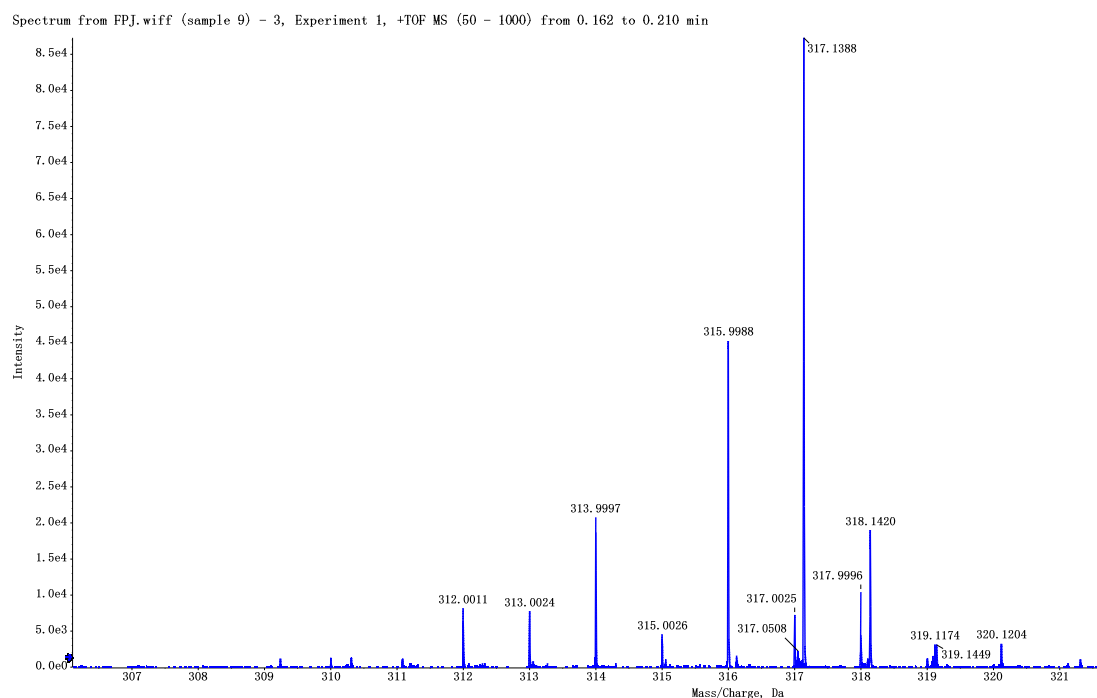
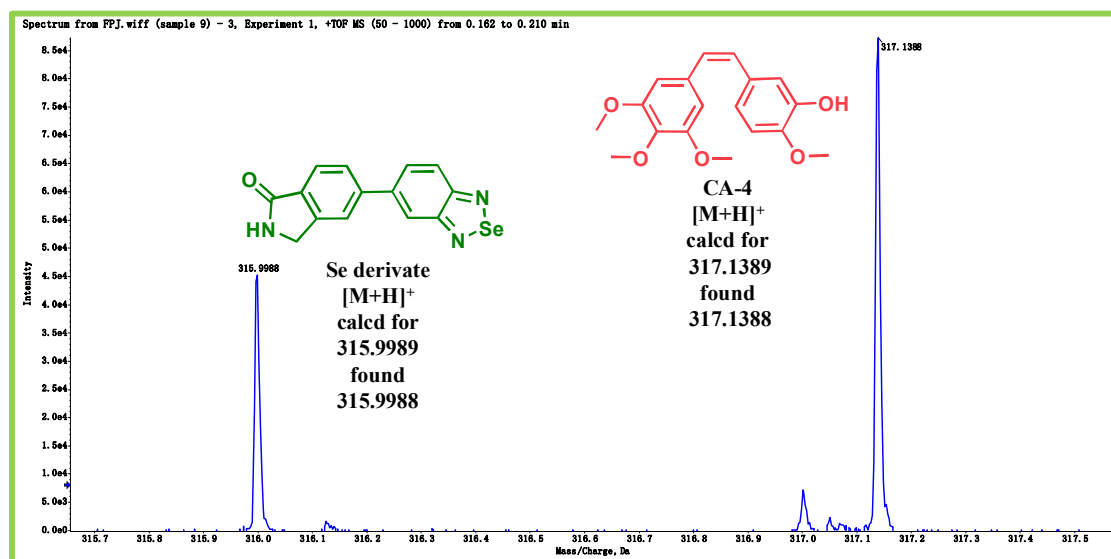


Fig. S27 ESI-MS of TPP-CSeD in PBS-DMSO solution initiating for 5 h.



Hit	Formula	m/z	RDB	ppm	MS Rank
1	C14H10N3OSe	315.9984	13.0	1.2	1
Hit	Formula	m/z	RDB	ppm	MS Rank
1	C18H21O5	317.1384	9.0	1.4	1

Fig. S28 Magnification certain parts of **Fig. S27**.

References

- S1 Huang Y., Luo Y., Zheng W., & Chen T, *ACS Applied Materials & Interfaces*, 20146(21), 19217-19228.
- S2 Chang Y., He L., Li Z., Zeng L., Song Z., Li P., & Chen, T, *ACS Nano*, (2017)11(5), 4848-4858.
- S3 Liu T., Lai L., Song, Z., & Chen, T. *Advanced Functional Materials*, 2016, 26(43), 7775-7790.
- S4 Huang Y., He L., Liu W., Fan C., Zheng W., Wong Y.-S., & Chen T, 2013, *Biomaterials*, 34(29), 7106–7116.
- S5 Zhang H., Ma Y., Sun, X.-L, *Chem. Commun.*, 2009, 3032-3034.
- S6 Ma Y, Zhang H, Sun XL, *Bioconjug Chem.* 2010;21(11):1994-1999.